Vietnam Journal of Earth Sciences, 45(1), 67-81, https://doi.org/10.15625/2615-9783/17581

Vietnam Journal of Earth Sciences
https://vjs.ac.vn/index.php/jse

Magnetotellurics study of Atambua area, West Timor, Indonesia

Edy Wijanarko[1,2], Ilham Arisbaya[1,3], Prihadi Sumintadireja[4], Warsa[1], Hendra Grandis[1*]

[1]*Faculty of Mining and Petroleum Engineering, Institut Teknologi Bandung (ITB), Indonesia*
[2]*Research Center for Oil and Gas "LEMIGAS", Indonesia*
[3]*National Research and Innovation Agency (BRIN), Indonesia*
[4]*Faculty of Earth Science and Technology, Institut Teknologi Bandung (ITB), Indonesia*

Received 15 August 2022; Received in revised form 5 October 2022; Accepted 13 October 2022

ABSTRACT

Timor Island, located in the eastern Indonesian archipelago, has a complex tectonic evolution causing complex geological structures. Many hypothetical tectonic models are proposed mainly based on regional geological and geophysical data. Available geophysical data to support geological study at a more detailed scale are still very limited. Therefore, this study aimed to map the sub-regional subsurface geology in Atambua, West Timor, and its surroundings by using the magnetotelluric (MT) method. The estimated geo-electrical strike direction from the phase tensor analysis confirmed the regional Southwest - Northeast general structural orientation. The dimensionality analysis also showed the validity for 2D approximation in that direction. The subsurface resistivity models from 2D inversion of the MT data at representative lines perpendicular to the regional structural direction delineate the primary sequences and their boundaries from their resistivities. They are, from top to bottom, Viqueque and Bobonaro sequences, Kolbano sequence, Kekneno sequence, and the basement dominated by rocks with Australian affinity. These main rock formations represent the regional sedimentary depositional fill resulting from the major tectonic events on Timor Island.

Keywords: Atambua, West Timor, 2D magnetotellurics, geoelectrical strike, phase tensor.

1. Introduction

The complex geology of Timor Island, Indonesia, and its surroundings (Fig. 1) is mainly influenced by the collision between the Northwest Australian Continental Plate and the Banda Island Arc due to the relative movement of the Australian Continent to the North. The tectonic activity has caused complicated geological and structural styles (Charlton et al., 1991; Nguyen et al., 2013) with the presence of a variety of rocks of various ages that are in contact with structures (Berry and McDougall, 1986; Harris and Long, 2000; Hall and Wilson, 2000). Various existing tectonic and geological models for Timor Island indicate that the area is interesting to study. They are also open to discussion on which concepts or models are most in line with the actual data (Harris, 1991; 2011; Audley-Charles, 2011). The complexity of Timor Island's tectonics has been the main subject of various publications, especially related to its hydrocarbon prospectivity, e.g., Charlton (2001); Lelono et al. (2016); Shaylendra et al. (2017), among others.

Generally, more quantitative subsurface information based on geophysical data is

*Corresponding author, Email: grandis@geoph.itb.ac.id

unavailable or poorly documented. Seismic surveys near Atambua and southwestern offshore West Timor were performed for hydrocarbon exploration (Jones et al., 2011; Bailie and Milne, 2014). The onshore seismic data are very limited in both lateral and depth coverage. The data are of poor quality, most probably due to strongly damped seismic waves by the near-surface layer, so the energy cannot probe into deeper subsurface layers. This led to difficulties in interpreting information on the study area's sedimentary layers and geological structures. The seismic reflection method usually produces a low signal-to-noise ratio in rough terrain areas formed by complex tectonics often manifested as overthrust faults (Mansfield et al., 2015). A previous gravity study around Atambua was carried out by Wijanarko et al. (2022) with the finding of Southwest - Northeast trending basins and the main sedimentary sequences filling the basins.

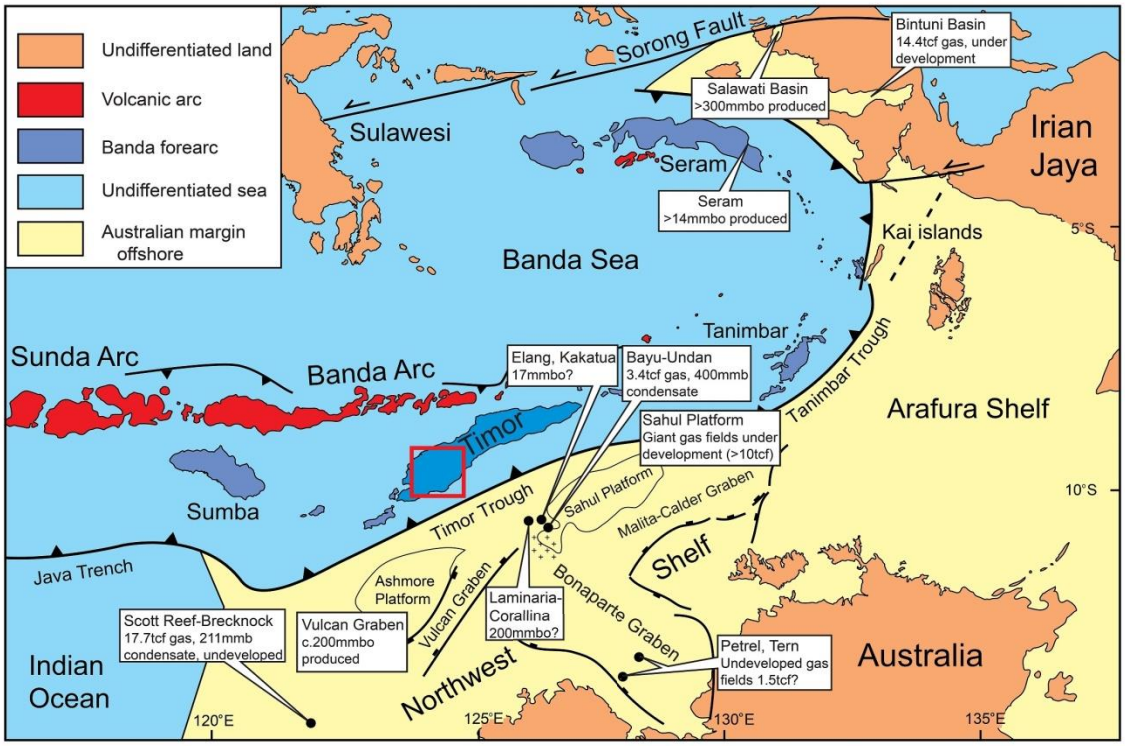

Figure 1. Location of Timor Island within the regional tectonics and hydrocarbon prospectivity context (after Charlton, 2001). The red box outlines approximately the study area.

This paper presents the results of a magnetotellurics (MT) study for subsurface geological mapping in the western part of the island, particularly near Atambua. The MT method employs natural electromagnetic (EM) fields to probe the subsurface and to infer rock formations based on their resistivity. The MT method has relatively good accuracy in predicting the depth and thickness of the subsurface layers, including the underlying basement and possibly structures that are generally more difficult to identify. The MT method can resolve complex structures in volcanic or limestone-covered and overthrust belt areas, where the seismic method is problematic (Patro, 2020; Xu et al., 2020; Palshin et al., 2020). The MT 2D modeling results are interpreted to infer the

subsurface geology of the study area, more particularly to delineate layer boundaries and the basement based on the resistivity models.

2. Geological Setting

Within the tectonic framework, Timor Island is located in the Outer Banda Arc (see Fig. 1). There are juxtaposing rocks affected by tectonic events. The oldest exposed sedimentary rocks in Timor Island are the Early Permian indicating the syn-rift phase. In general, many authors conclude that the oldest sedimentary rocks were deposited in a marine environment (Charlton et al., 1991; Harris, 2011; Audley-Charles, 2011; Charlton, 2001; Villeneuve et al., 2013; Sawyer et al., 1993). However, Lelono et al. (2016) consider the lacustrine setting. Even so, they agree that the origin of Timor Island comes from the Gondwana mega-continent. The syn-rift phase in Timor Island deposited very fine grain materials of shale to fine sandstone, carbonaceous rock clastic or reef, and volcanic rock during rifting. The final stage of syn-rift is indicated by changing environmental deposition to deep water marine and a hiatus of unconformity overlying post-rift sequence in the Upper Jurassic. The unconformity was affected by the break-up of Timor Island from the Gondwana mega-continent in 155 Ma (Hall and Wilson, 2000).

The depositional products after syn-rift are post-rift or Kolbano sequences that began in Cretaceous to Early Miocene. Tectonic events at this stage were relatively more stable than at the other phases. The post-rift sequence, generally, has sedimentation patterns shallowing upward sedimentation patterns that are changing the depositional environment from a distal area, i.e., a deep-sea sedimentation environment, to a proximal depositional environment, consisting of transition to the terrestrial area. This can be seen from the deposition of the Nakfunu Formation, which appears as chalky and calculative, underlying the Ofu Formation, which consists of calcarenite (Charlton, 2001). At the end of the post-rift phase, Timor Island moves toward the North of Gondwana mega-continent.

The final stage of tectonic events in Timor Island is a collision. This phase consists of syn-orogeny and post-orogeny with identical lithologies. The exposed rocks constitute gravel, calcareous rock, and alluvial. These rocks were deposited during Late Tertiary to Pleistocene, commonly in a shallow marine setting. The tectonic events at this phase are very active, resulting in massive deformations in Timor Island, such as thrusting, folding, inversion structure, mud diapirism, and obduction (see Fig. 2). The massive tectonics controls basin configuration in different ways at West Timor and East Timor. The characteristics of West Timor basins are wide and circular, while the East Timor basins are narrower and more elongated (Charlton et al., 1991; Charlton, 2001).

Based on the rifting process described earlier, the regional stratigraphy in Atambua, West Timor, and its surrounding can be grouped into three sequences, namely the Kekneno sequence, the Kolbano sequence, and the Viqueque sequence. Sawyer et al. (1993) divided the Kekneno sequence into various rock formations, namely: Bisane (Atahoc and Cribas), Maubisse, Niof, Aitutu, Babulu, and Wailuli formations. The Kolbano sequence consists of the Oebaat, Nakfunu, Menu, and Ofu formations. The Viqueque sequence is composed of Viqueque (Batuputih and Naole) and coral limestone, and alluvium formations. The other rock that exists there comes from Banda-Arc, so-called allochthonous referred to as its sedimentary rock and Banda terrane in terms of the whole rocks.

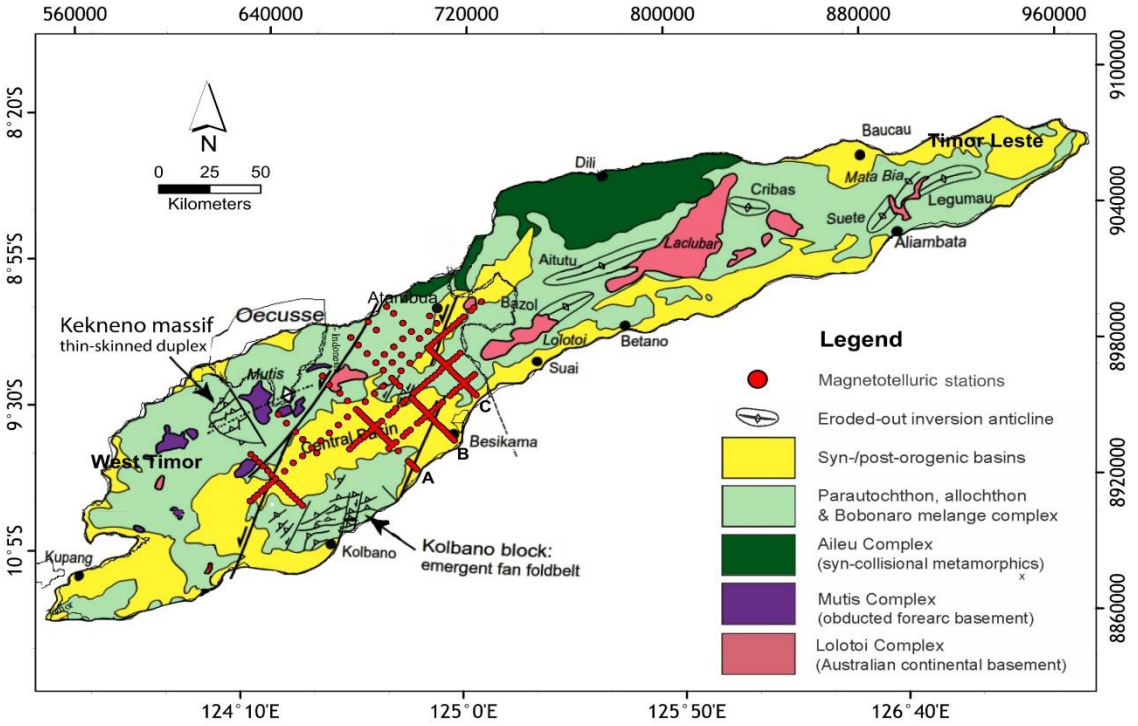

Figure 2. Simplified structural map and metamorphic complexes of Timor Island from Charlton (2001) overlaid with magnetotelluric (MT) data acquisition stations distributed along traverse lines. The 2D MT modeling was performed for three main profiles, A, B, and C.

3. Magnetotelluric (MT) Method

The magnetotelluric (MT) method is a passive geophysical technique that uses natural electromagnetic (EM) fields to infer the subsurface electrical conductivity (or resistivity) distribution. The transient variations of the Earth's magnetic field are due to its interaction with the solar wind and thunderstorms that mostly occur in equatorial regions. The induced electric field in the Earth's interior depends largely on the electrical properties of the lithosphere (Simpson and Bahr, 2005). One of the advantages of the MT method is its deep investigation depth, related to the wide frequency band of the EM induction phenomenon, mostly from 0.0001 Hz to 1000 Hz. The resistivity variations of rocks cover a broad range, although many of them overlap. Therefore, MT primarily applies to regional and sub-regional scale subsurface investigations associated with basin and prospect scale studies, respectively (Patro, 2020).

During a typical MT sounding, electric and magnetic field components are measured from electrode pairs and magnetic induction coils, respectively. The raw time series data are recorded digitally in the main unit of the data acquisition system. In the frequency domain, horizontal components of the electric (E_x, E_y) and magnetic (H_x, H_y) fields are related through the impedance tensor, while the vertical magnetic component (H_z) is related to its horizontal counterparts (H_x, H_y) by the-so-called tipper vector. In MT data processing, the time series data are first transformed into the Fourier domain to calculate their power spectra, then the transfer functions between measured field components are estimated (Simpson and Bahr, 2005; Epishkin, 2016).

The transfer functions contain information on the subsurface resistivity distribution. However, further analysis is needed before such information can be extracted. Conventional analysis of the impedance tensor usually consists of a simple rotation of the tensor's coordinate system to obtain principal tensor components typical of a 2D structure. A more robust method includes phase tensor analysis (Caldwell et al., 2004) to infer the dimensionality of the subsurface conductivity structure, i.e., geo-electrical strike, and whether the data can be of 2D or more complex 3D structures. The major axis (α - β) of the phase tensor of MT data determines the regional strike, while low skew angle values, i.e., typically $-3^o < \beta < 3^o$, indicate that the subsurface can be considered as 2D. Hence, the 2D MT inversion modeling is applicable.

The real subsurface structures are rarely 2D. Nevertheless, 3D MT inversion modeling to obtain realistic 3D resistivity distribution of the subsurface is relatively costly and time-consuming. Therefore, 2D MT modeling is still routinely performed, despite the availability of 3D modeling codes practically free for academic purposes. The lack of computational resources often hinders 3D MT modeling on a routine basis. In 2D MT modeling, careful data analysis and selection may result in reliable 2D resistivity models describing the geology of the study area. In this paper, we used the non-linear conjugate gradient (NLCG) algorithm (Rodi and Mackie, 2001) performed within the well-known WinGLink software from Geosystem (Geosystem Ltd, 2008) to obtain a resistivity model at three main sections perpendicular to the regional strike (Charlton et al., 1991; Charlton, 2001). The modeling starts with an initial homogeneous model that is updated iteratively while minimizing an objective function containing misfit and model "roughness" terms. The latter is intended to obtain a smooth resistivity model of the subsurface. We chose the regularization parameter such that there is a good balance between low misfit and model smoothness, which is geologically feasible and consistently explains the observed data.

4. Results

The magnetotelluric (MT) survey was done at 90 sounding sites with 0.5 to 1 km intervals between stations along traverse lines, as well as farther spacings at the profiles' ends as shown in Fig. 2. At each MT station, the time series data were recorded for at least 12 hours by using MTU-5A Phoenix Geophysics data acquisition system. The duration was more than adequate to ensure relatively good quality data for low-frequency MT. For the audio-frequency band MT (AMT), the data recording was only about 1 hour before overnight measurement for lower frequency bands. The broadband MT data covered a frequency range of 0.001-10000 Hz, sufficient to probe approximately up to 10 km depth. The Differential Global Positioning System (DGPS) measurements position all MT sounding stations.

The recorded time series data were processed to obtain power spectra of all channels associated with components of electric and magnetic fields. We used a spectral coherency threshold value greater than 0.75 to ensure reliable data, followed by a selection of power spectra and combination AMT-MT frequency bands. The MT data processing was performed by using the software provided by the equipment's manufacturer, i.e., SSMT-2000 and MT-Editor from Phoenix-Geophysics (Phoenix-Geophysics Inc, 2005). The transfer functions obtained from the data processing were subjected to further directional and dimensional analyses.

The results of the phase tensor analysis (Caldwell et al., 2004) for all MT data show

that the major axis (α - β) associated with the geo-electrical strike has a wide spread between N60°W and N60°E for a short period range from 0.0001 to 10 sec. The absence of a dominant geo-electrical strike direction is due to layered structures that usually prevail in the shallower parts of the basin. For the longer period range from 10 sec. or more, the geo-electrical strike is more definitive as N30°W, indicating the influence of the deeper parts of the basin (Fig. 3). However, the geo-electrical strike always has ± 90° ambiguity that can be resolved by the tipper strike (Simpson and Bahr, 2005). The latter shows that the structural direction may also be around N60°E which is in good agreement with the regional geology having NE-SW trends (Charlton et al., 1991; Charlton, 2001). Therefore, the MT impedance tensor was rotated to N60°E, and the off-diagonal principal components obtained were used in the 2D MT modeling.

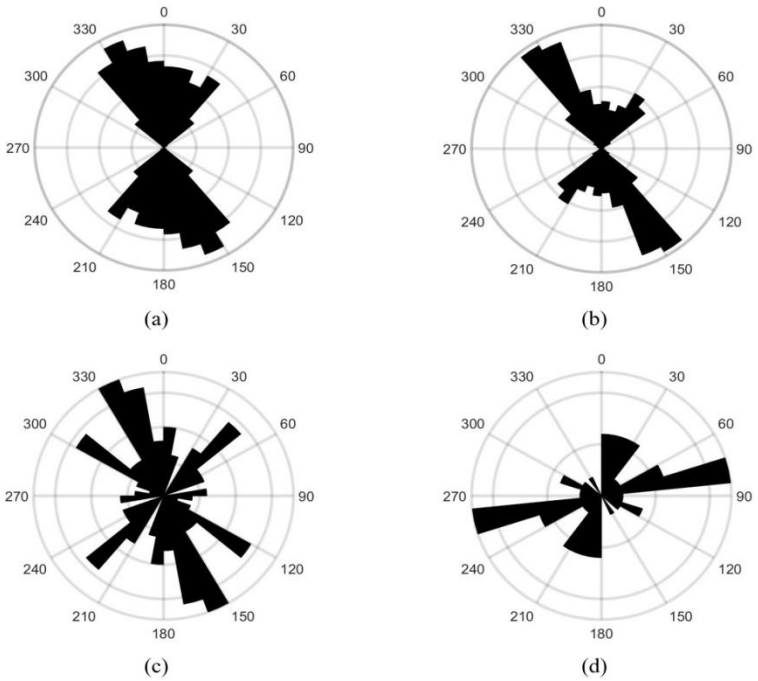

Figure 3. Rose diagrams summarizing the geoelectrical strike estimation from phase tensor analysis for the period range (a) 0.0001 to 10 sec. (b) 10 to 1000 sec. and rose diagrams showing tipper strike estimation for the period range (c) 0.0001 to 10 sec. (d) 10 to 1000 sec.

Another fundamental parameter from the impedance tensor analysis using phase tensor analysis is the skew angle (β) which indicates the dimensionality of the conductivity structure. The structure is considered to be 2D when $-3^{o} < \beta < 3^{o}$ (Caldwell et al., 2004), which is the case for the MT data, especially at three main traverse lines, designated as line AA' (A), BB' (B) and CC' (C) (see Fig. 2), that will be further modeled. There are exceptions at some very short periods, probably due to local superficial distortions, and also at periods longer than 200 sec. that may be related to the low signal-to-noise ratio of the long-period EM fields (Fig. 4). Nevertheless, from the remaining period range valid for 2D modeling, i.e., 0.0001 to 100 sec., we expect that the MT data would be beneficial in obtaining overall subsurface resistivity structure of the area at a regional or sub-regional scale as was proven in another similar case with less dense MT stations

distribution (e.g. Irawati et al., 2022). Rose diagrams and skew angle β for MT stations at lines AA', BB', and CC' are summarized in Fig. 5. Along with the geological map of Atambua, mud volcano, and oil and gas seeps are also shown in Fig. 5.

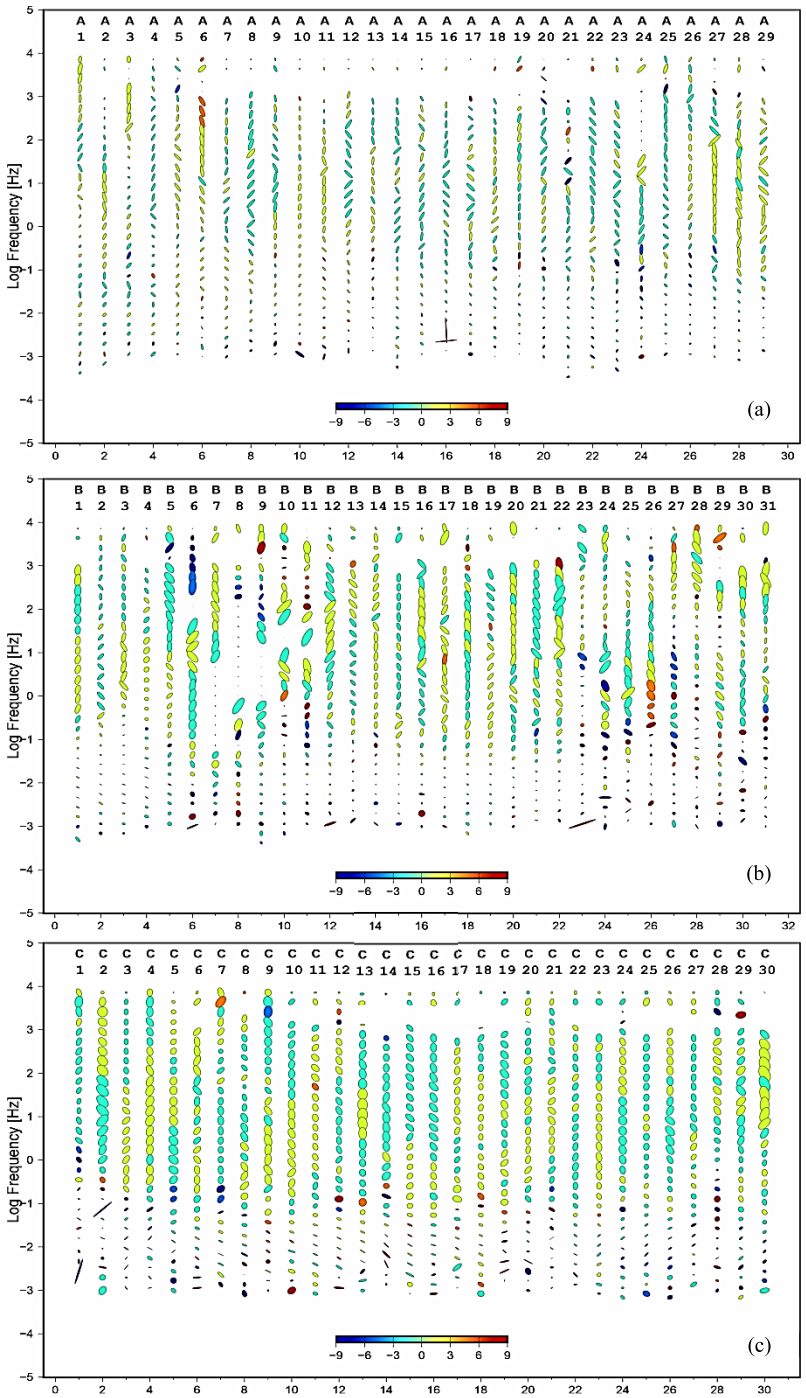

Figure 4. Phase tensor analysis results show principal directions as ellipses and skew angle β in colors for three main profiles AA', BB' and CC' in (a), (b), and (c), respectively.

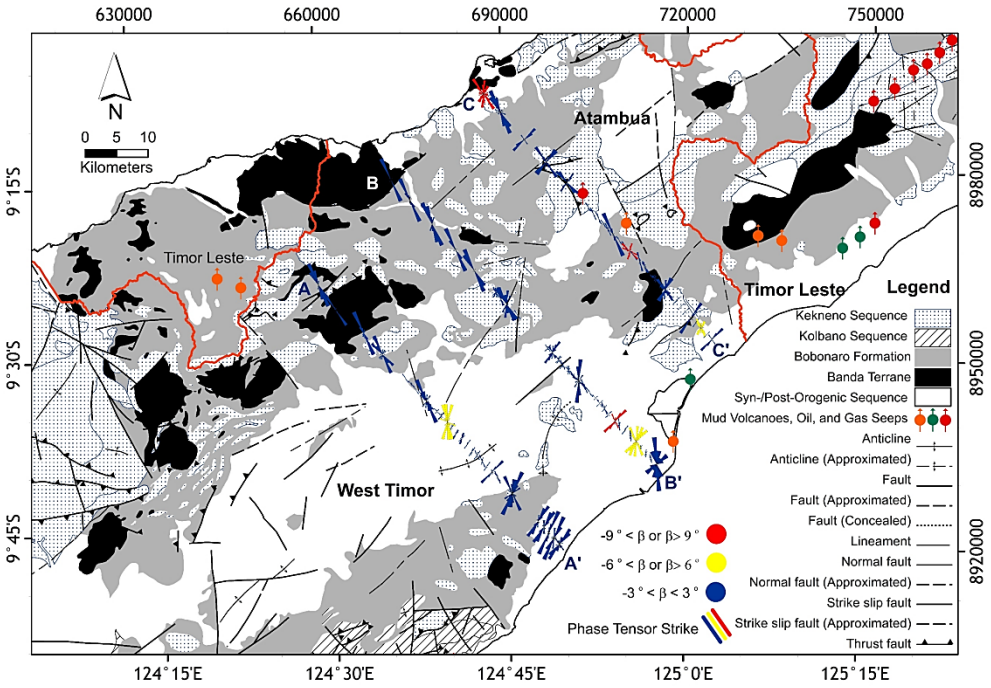

Figure 5. Rose diagrams for the period range 10 to 1000 sec. and skew angle β for 1 sec. Estimated from phase tensor analysis of MT stations at three main profiles AA', BB' and CC' overlaid on the geological map of the Atambua area.

In 2D MT inversion modeling, a 2D mesh was created with a combination of fine and coarser meshes at denser (around 500 meters) and at sparse (more than 1000 meters) sounding station areas. We used the default 100 Ohm.m homogeneous medium as the starting model. It is well-known that geophysical modeling is generally unstable, and the solution is non-unique. Additional constraints are used in the search for an optimal model. Therefore, minimizing the objective function consists of the misfit function and a regularization term. The latter is a spatial variation of the model parameters such that the model would be smooth. To find an appropriate regularization parameter τ for trade-off between misfit and model smoothness, we carried out an inversion of MT data with different τ values. The resulting L-shaped trade-off curve was used to choose the optimal τ parameter (Hansen, 2001). The regularization parameter τ = 15 was selected as the appropriate value for all inversions (Fig. 6). In addition, we used horizontal smoothing $\alpha = 3$ to emphasize layering, while $\beta = 1$ for parameters that govern the smoothing factor (Geosystem Ltd, 2008). The final inverse models were derived after a minimum of 30 iterations for joint inversion of TE-mode and TM-mode data.

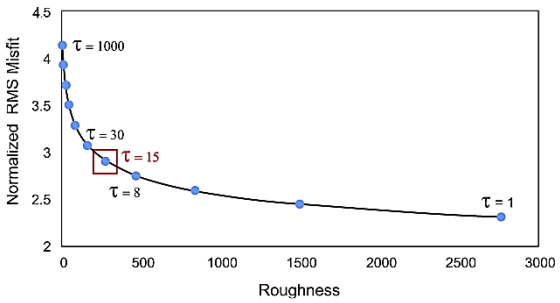

Figure 6. The L-shaped trade-off curve plots of RMS errors against model roughness for different values of regularization parameter τ.

The iterative model adjustments resulted in sufficiently smooth resistivity models while maintaining their discrimination to delineate

the main subsurface formations based on their resistivity contrasts. The 2D MT inversion modeling results for line AA', BB', and CC' perpendicular to the regional strike are presented in Fig. 7. At all profiles, the superficial layer up to 2-3 km depth is characterized by very low resistivity values, i.e., less than 5 Ohm.m. Underneath is a moderately low resistivity layer between 10 to 50 Ohm.m at 2 to 4 km depth. The transition layer to a more resistive basement (more than 500 Ohm.m at 5 to 6 km depth) is a relatively thin layer, especially at line AA' with a resistivity of 100 to 300 Ohm.m (see Fig. 7).

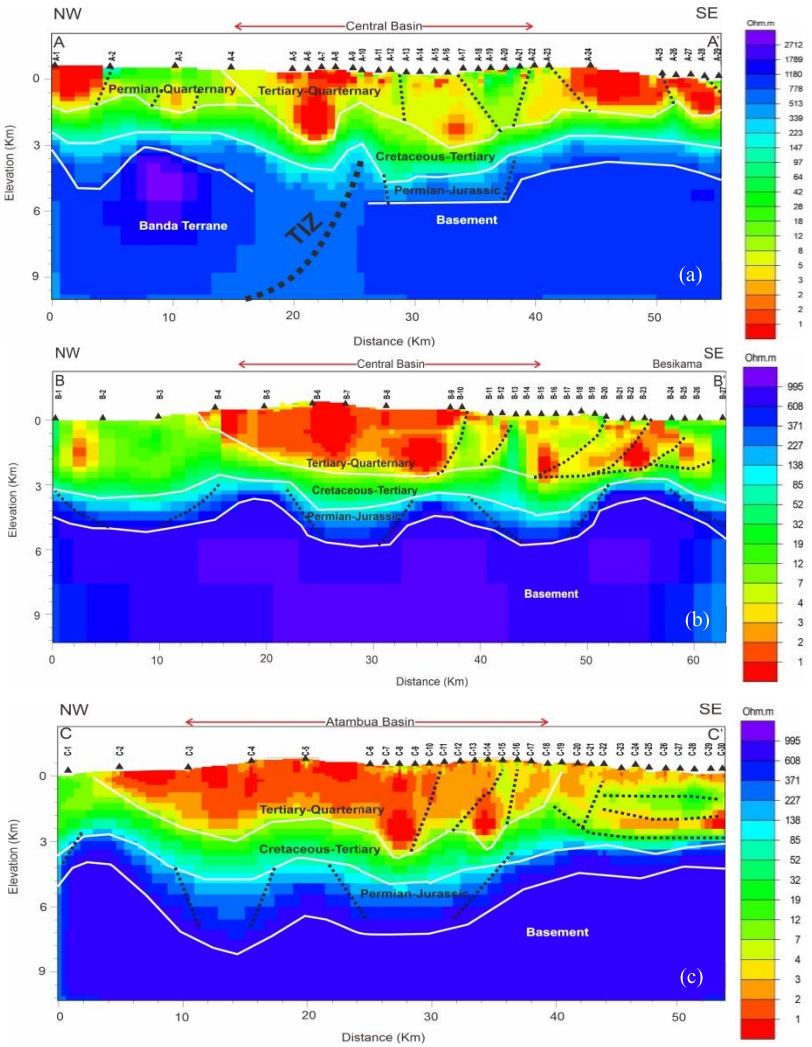

Figure 7. Resistivity sections from 2D MT inversion modeling for three main profiles AA', BB' and CC' in (a), (b), and (c), respectively. White continuous lines are sequence boundaries and black dashed lines are interpreted faults (see Discussion for more details)

The RMS error between observed and calculated data for models at line AA', BB' and CC' are 2.63, 2.46, and 1.82, respectively. They can be considered as acceptable given the typical noise of MT data from equatorial regions (Padilla, 1999; Chave and Jones, 2012). In general, there is a good agreement between observed and calculated data presented as apparent resistivity and pseudo phase sections, as shown in Fig. 8, Fig. 9, and Fig. 10 for line AA', BB', and CC,' respectively.

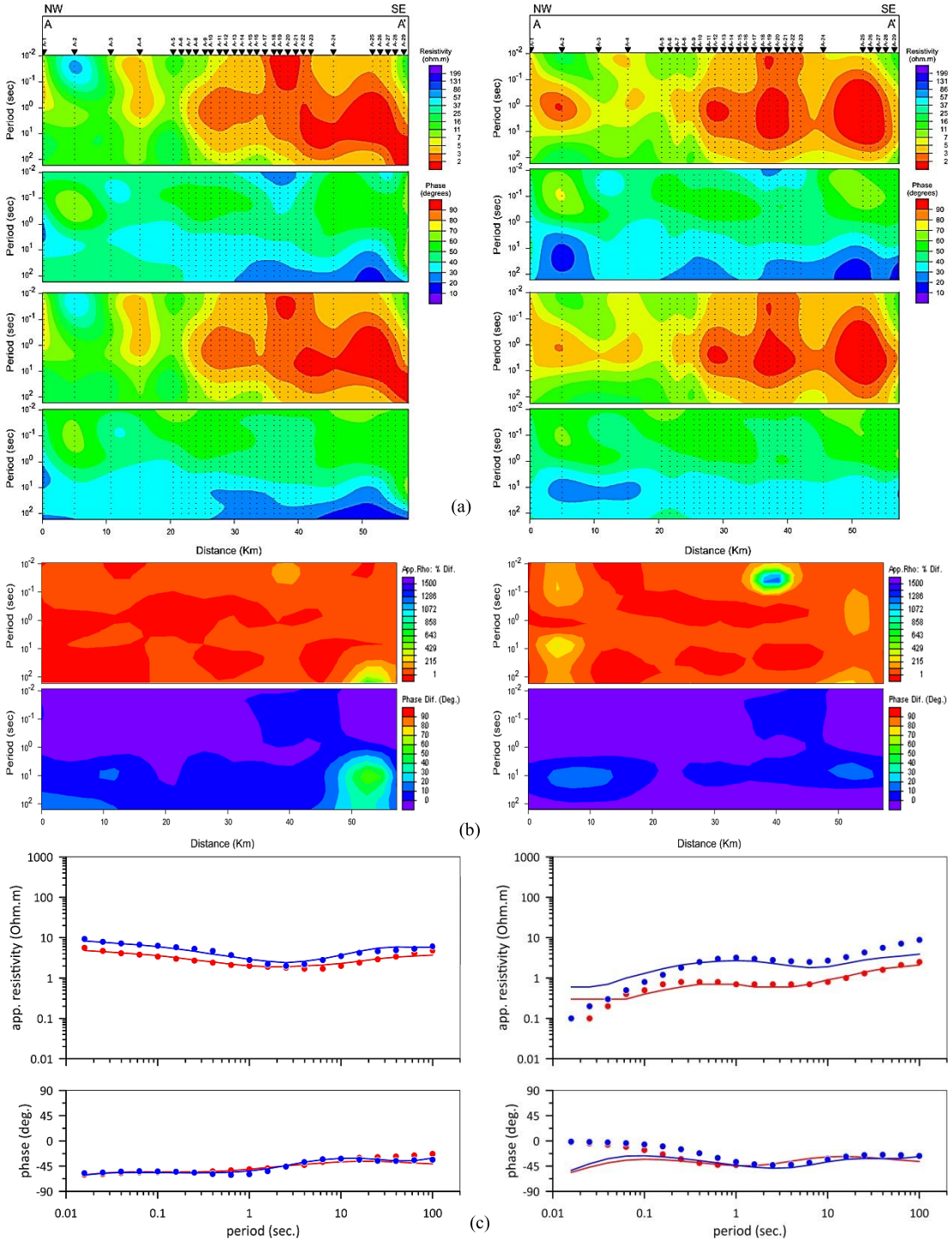

Figure 8. (a) Apparent resistivity and phase pseudosections of observed (top) and calculated (bottom) from 2D MT inversion for profile AA', TE-mode (left panel), and TM-mode (right panel), (b) Sections for differences between measured and calculated data shown in (a), (c) Sounding curves of measured (circle) and calculated data (line) for the best match (left panel, station A-8) and the worst match (right panel, station A-19), TE-mode (red) and TM-mode (blue)

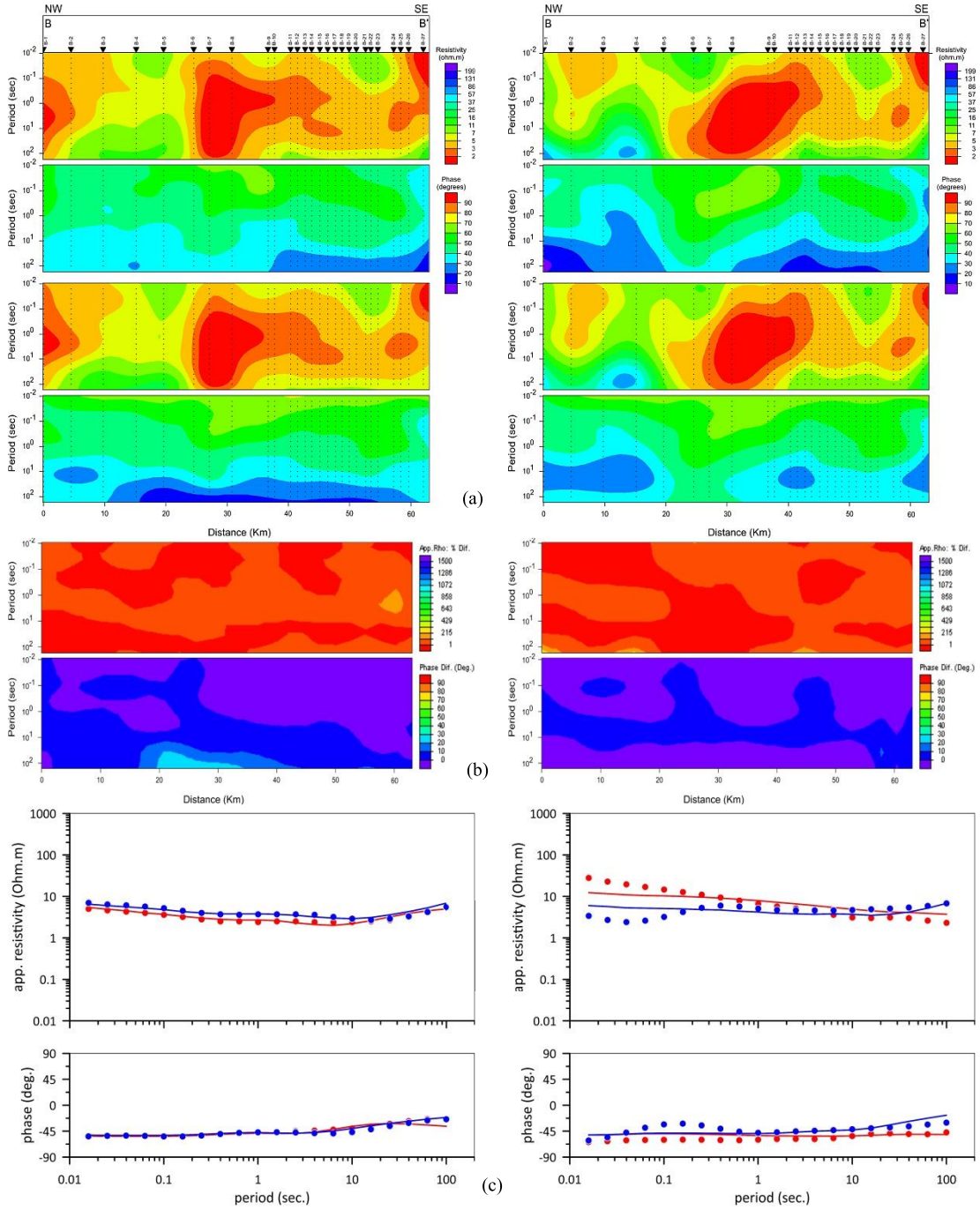

Figure 9. (a) Apparent resistivity and phase pseudosections of observed (top) and calculated (bottom) from 2D MT inversion for profile BB', TE-mode (left panel), and TM-mode (right panel), (b) Sections for differences between measured and calculated data shown in (a), (c) Sounding curves of measured (circle) and calculated data (line) for the best match (left panel, station B-6) and the worst match (right panel, station B-26), TE-mode (red) and TM-mode (blue)

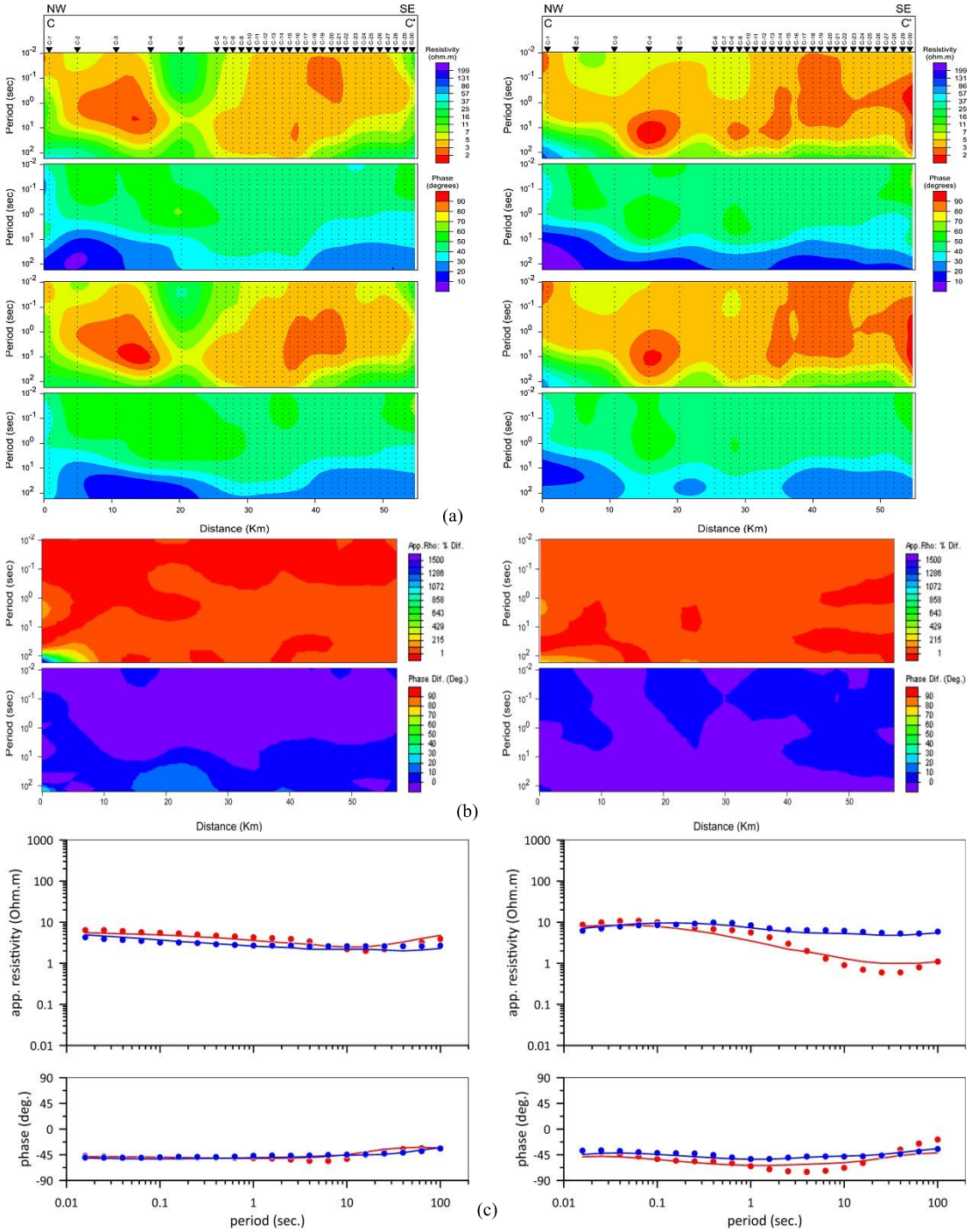

Figure 10. (a) Apparent resistivity and phase pseudosections of observed (top) and calculated (bottom) from 2D MT inversion for profile CC', TE-mode (left panel), and TM-mode (right panel), (b) Sections for differences between measured and calculated data shown in (a), (c) Sounding curves of measured (circle) and calculated data (line) for the best match (left panel, station C-10) and the worst match (right panel, station C-8), TE-mode (red) and TM-mode (blue)

5. Discussions

The subsurface resistivity models from MT data at line AA', BB', and CC' shown in Fig. 7 represent the regional and sub-regional sedimentary depositional fill resulting from the main tectonic events that occurred on Timor Island. The uppermost very conductive layer (less than 5 Ohm.m) is heterogeneous, especially at line AA' with non-continuous layering appearance. This less compact layer represents the Viqueque sequence (Tertiary to Quaternary) and Bobonaro mélanges (Tertiary) dominating the surface of the study area. The Viqueque sequence is dominated by coral-limestone, conglomerates, and alluvium deposits which are mostly exposed in the central area or Central basin and the East-Northeast area, while the Bobonaro mélanges consist of various matrices of clay and shale (Harris, 2011; Audley-Charles, 2011).

The second (around 10 to 50 Ohm.m) and third (about 100 to 300 Ohm.m) layers which are moderately conductive, can be associated with Kolbano and Kekneno sequences, i.e., post-rift (Cretaceous-Tertiary) and syn-rift (Permian-Jurassic) sequences, respectively. Carbonaceous rocks dominate the Kolbano sequence from calcilutite, calcarenite, and calcirudite. The Kekneno sequence combines shale and carbonaceous rocks with additional members having lithologies from shale to sandstone, calcareous and volcanic rocks (Harris, 2011; Sawyer et al., 1993). Lastly, the lowermost resistive layer is interpreted as the basement (more than 500 Ohm.m). For line AA' (see Fig. 7a), there is a minor resistivity difference in the basement, where the Northwestern part is slightly more resistive than the southeastern part. This discontinuity may indicate the position the Tectonic Inversion Zone (TIZ) that separates the basement from two different provenances, i.e. the Northwestern part is Banda terrane, while the southeastern part is the Australian basement (Harris, 2011).

The interpretation for the resistivity section at line BB' is quite similar to that of line AA' with minor exceptions concerning the continuity of the layers. The superficial, shallow resistivity layer appears more continuous at line BB', especially in the Central basin area. Although with insignificantly lower resistivity, the resistive basement is also more continuous than line AA' (see Fig. 7b). In this area, the layer representing the basement is associated with Australian affinity (Harris, 2011). The resistivity model for line CC' and its interpretation are similar to those of line BB'. However, some features are geometrically different. The uppermost very conductive layer representing the basin is more extensive and more profound than the Central basin in line AA' and line BB'. In this area the basin is associated with the Atambua basin. Consequently, the basement is also deeper, extending to 6 km depth (see Fig 7c). The development of the basins is controlled by the trans-tension force associated with the left-lateral strike-slip fault (see Fig. 2) (Charlton et al., 1991).

The average thickness of the para-autochthons (syn- and post-rift sequences) at line CC' is about 4 Km, while at line BB' and line AA' they are about 3 Km. There is a possibility that a hydrocarbon system exists in the Atambua area, West Timor, and its surroundings. This refers to the Aitutu Formation, which has been proven to produce hydrocarbons and can release oil and gas (Shaylendra et al., 2017), and Charlton (2001) identified the Wailuli Formation (shale dominance) as a regional seal on the island of Timor. Those Mesozoic sediments can form a petroleum system play as many carbonates or sandstone of Kekneno, and Kolbano sequences can be reservoir rocks. There is also an anticline structure as a trap of hydrocarbon.

Additionally, the Mesozoic sediment has the most significant thickness compared to the

Paleozoic and Cenozoic sediments. The presence of hydrocarbons in the Mesozoic play is probably at the crest and limp of the anticline and the anticline that experienced inversion. The area is located in the Central and eastern parts of line AA', line BB' and line CC'.

6. Conclusions

The magnetotellurics (MT) study at Atambua and its surroundings show that the main sequences and their boundaries can be clearly recognized based on their resistivities. In general, there are four sequences identified, i.e. the pre-rift representing the Australian basement, the syn-rift associated with the Kekneno sequence, the post-rift depicting the Kolbano sequence, and the orogeny phase revealed by the Viqueque sequence. In addition to the Australian basement, there is also a juxtaposed Banda terrane with an overlying allochthonous layer recognized in the Northwestern part of the area. The existence of the two main basins in the study area is also emphasized, i.e., the Central basin and the Atambua basin. However, their geometry might be different from those previously revealed by geological data (see Fig. 2) (Charlton, 2001).

This paper focuses more on the existing subsurface formations rather than the tectonic process that might produce those features. The extension of our results to explain the tectonic activities that have occurred is beyond this paper's scope. Nonetheless, our results with MT data corroborate the main results from gravity data (Wijanarko et al., 2022). Hence, it can be concluded that the thick sediments from the pre-collisional events can be associated with the former Northwestern part of the Australian passive margin. The latter has been identified from previous surface geological data as good petroleum system elements, i.e., source and reservoir rocks (Charlton, 2001; Shaylendra et al., 2017; Surjono et al., 2017). This research provides a location where prospect areas for hydrocarbon potential should be further explored, i.e., the Central basin and Atambua basin. Integrated analysis of 3D gravity and MT 2D modeling is ongoing to obtain more comprehensive and confident results.

Acknowledgments

The authors acknowledge the Center for Oil and Gas "LEMIGAS" for the permission to publish the data, the Ministry of Energy and Mineral Resources of Indonesia for a scholarship awarded to E. Wijanarko, and Institut Teknologi Bandung for P2MI grant 2022 to H. Grandis.

References

Audley-Charles M.G., 2011. Tectonic post-collision processes in Timor. Geol. Soc. London Spec. Pub., 355, 241-266. https://doi.org/10.1144/SP355.12.

Bailie P., Milne C., 2014. New insights into prospectivity and tectonic evolution of the Banda Arc: Evidence from broadband seismic data. Proc. 38th Indonesian Petrol. Assoc. (IPA) Ann. Conv., Jakarta, Indonesia.

Berry R.F., McDougall I., 1986. Interpretation of 40Ar/39Ar and K/Ar dating evidence from the Aileu Formation, East Timor, Indonesia. Chem. Geol. Isot. Geosci. Sect., 59, 43-58. https://doi.org/10.1016/0168-9622(86)90056-4.

Caldwell T.G., Bibby H.M., Brown C., 2004. The magnetotelluric phase tensor. Geophys. J. Int., 158, 457-469. https://doi.org/10.1111/j.1365-246X.2004.02281.x.

Charlton T.R., Barber A.J., Barkham S.T., 1991. The structural evolution of the Timor collision complex, eastern Indonesia. J. Struct. Geol., 13, 489-500. https://doi.org/10.1016/0191-8141(91)90039-L.

Charlton T.R., 2001. The petroleum potential of West Timor. Proc. 28th Indonesian Petrol. Assoc. (IPA) Ann. Conv., Jakarta, Indonesia.

Chave A., Jones A., 2012. The Magnetotelluric Method: Theory and Practice. Cambridge University Press.

Epishkin D.V., 2016. Improving magnetotelluric data processing methods. Moscow Univ. Geol. Bull., 71, 347-354. https://doi.org/10.3103/S0145875216050057.

Geosystem Ltd., 2008. WinGLink User's Guide, Release 2.20.02.01.

Hall R., Wilson M.E.J., 2000. Neogene sutures in eastern Indonesia. J. Asian Earth Sci., 18, 781-808. https://doi.org/10.1016/S1367-9120(00)00040-7.

Harris R., 1991. Temporal distribution of strain in the active Banda orogen: a reconciliation of rival hypotheses. J. Southeast Asian Earth Sci., 6, 373-386. https://doi.org/10.1016/0743-9547(91)90082-9.

Harris R., 2011. The nature of the Banda Arc - Continent Collision in the Timor region, In: Brown D, Ryan PD. (eds.) Arc-Continent Collision, Frontiers in Earth Sciences, Springer, 163-211. https://doi.org/10.1007/978-3-540-88558-0_7.

Harris R., Long T., 2000. The Timor ophiolite, Indonesia: Model or myth? Geol. Soc. America Spec. Papers, 349, 321-330.

Hansen P.C., 2001. The L-curve and Its Use in the Numerical Treatment of Inverse Problems. WIT Press.

Irawati S.M., Hidayat, Wijanarko E., Grandis H., 2022. Integrated magnetotellurics (MT), gravity and seismic study of lower Kutai Basin configuration. J. Eng. Technol. Sci., 54, 220103. https://doi.org/10.5614/j.eng.technol.sci.2022.54.1.3.

Jones W., Tripathi A., Rajagopal R., Williams A., 2011. Petroleum prospectivity of the West Timor Trough. PESA News, 114, 6-10.

Lelono E.B., Bohemi P., Bachtiar A., Suandhi P., Utomo B.H., Ibadurrahman H., Arifai M., Yusliandi A., Lesmana Z., 2016. Paleozoic lacustrine sediment at West Timor and tectonic implication for Timor Island: New exploration concept of hydrocarbon. Proc. 40th Indonesian Petrol. Assoc. (IPA) Ann. Conv., Jakarta, Indonesia.

Mansfield G., Chandra S., Carver P., 2015. Where's the data? Acquisition and processing of seismic data in the PNG highlands. AAPG/SEG Inter. Conf. Exhib., Melbourne, Australia.

Nguyen N., Duffy B., Shulmeister J., Quigley M., 2013. Rapid Pliocene uplift of Timor. Geology, 41, 179-182. https://doi.org/10.1130/G33420.1.

Padilla A.L., 1999. Behaviour of magnetotelluric source fields within the equatorial zone. Earth Planets Space, 51, 1119-1125. https://doi.org/10.1186/BF03351585.

Palshin N., Giraudo R.E., Yakovlev D., Zaytsev S., Aleksanova E., Zaltsman R., Korbutiak S., 2020. Detalied magnetotelluric study of the northern part of Subandean fold belt, Bolivia. J. App. Geophys., 181, 104136. https://doi.org/10.1016/j.jappgeo.2020.104136.

Patro P.K., 2020. Magnetotelluric studies for hydrocarbon and geothermal resources: Examples from the Asian region. Surv. Geophys., 38, 1005-1041. https://doi.org/10.1007/s10712-017-9439-x.

Phoenix-Geophysics Inc., 2005. SSMT-2000 and MT-Editor Users' Manual.

Rodi W., Mackie R.L., 2001. Non-linear conjugate algorithm for 2-D magnetotelluric inversion. Geophysics, 66, 174-187. https://doi.org/10.1190/1.1444893.

Sawyer R.K., Sani K., Brown S., 1993. The stratigraphy and sedimentology of West Timor, Indonesia. Proc. 22nd Indonesian Petrol. Assoc. (IPA) Ann. Conv., Jakarta, Indonesia.

Shaylendra Y., Adlan Q., Kesumajana A.H.P., 2017. Petroleum system play failure on Triassic source rock in the west Timor onshore area: Basin modeling and oil to source rock correlation. Proc. 41st Indonesian Petrol. Assoc. Ann. Conv. (IPA), Jakarta, Indonesia.

Simpson F., Bahr K., 2005. Practical Magnetotellurics. Chambridge University Press.

Surjono S.S., Hidayat R., Wagimin N., 2017. Triassic petroleum system as an alternative exploration concept in offshore western Timor, Indonesia. J. Petrol. Explor. Prod. Tech., 8, 703-711. https://doi.org/10.1007/s13202-017-0421-4.

Villeneuve M., Bellon H., Martini R., Harsolumakso A.H., Cornée J.J., 2013. West Timor: A key for the eastern Indonesian geodynamic evolution. Bull. Soc. Géol. France, 184, 569-582. https://doi.org/10.2113/gssgfbull.184.6.569.

Wijanarko E., Arisbaya I., Sumintadireja P., Warsa W., Grandis H., 2022. Basin study in Atambua, West Timor, Indonesia from Gravity Data. J. Math. Fund. Sci., 54, 138-150. https://doi.org/10.5614/j.math.fund.sci.2022.54.1.8.

Xu Z., Xu Q., Liu A., Wang N., Li G., Peng C., Yan L., Su Y., 2020. The Cretaceous stratigraphy, Songliao Basin, Northeast China: Constrains from drillings and geophysics. Open Geosci., 12, 1212-1223. https://doi.org/10.1515/geo-2020-0188.